Received <day> <Month>, <year>; | Revised <day> <Month>, <year>; | Accepted <day> <Month>, <year>

DOI: xxx/xxxx

JOURNAL

Study of Input Space for State Estimation of High-Rate Dynamics

Jonathan Hong*[1,2] | Simon Laflamme[2] | Jacob Dodson[3]

[1]Applied Research Associates, Emerald Coast Division, Florida, USA
[2]Iowa State University, Civil, Construction, and Environmental Engineering, Iowa, USA
[3]Air Force Research Laboratory, Munitions Directorate, Florida, USA

Correspondence
*Jonathan Hong, Iowa State University, Ames, IA 50011. Email: jhong1@iastate.edu

Present Address
956 W. John Sims Pkwy Niceville, FL 32578

Abstract

High-rate dynamic systems are defined as systems being exposed to highly dynamic environments that comprise high-rate and high-amplitude events. Examples of such systems include civil structures exposed to blast, space shuttles prone to debris strikes, and aerial vehicles experiencing in-flight changes. The high-rate dynamic characteristics of these systems provides several possibilities for state estimators to improve performance, including a high potential to reduce injuries and save lives. In this paper, opportunities and challenges that are specific to state estimation of high-rate dynamic systems are presented and discussed. It is argued that a possible path to design of state estimators for high-rate dynamics is the utilization of adaptive data-based observers, but that further research needs to be conducted to increase their convergence rate. An adaptive neuro-observer is designed to examine the particular challenges in selecting an appropriate input space in high-rate state estimation. It is found that the choice of inputs has a significant influence on the observer performance for high-rate dynamics when compared against a low-rate environment. Additionally, misrepresentation of a system dynamics through incorrect input spaces produces large errors in the estimation which could potentially trick the decision making process in a closed loop system in making bad judgments.

KEYWORDS:
High-rate, Microsecond, Millisecond, State Estimation, Observers, Fast Dynamics

1 | INTRODUCTION

High-rate dynamic systems are systems being exposed to highly dynamic environments which comprise of high-rate and high-amplitude events. When exposed to these highly dynamic events, a system can undergo rapid changes. Examples of such systems include hypersonic vehicles and impact protection systems. The ability of an estimator to sense, analyze, and predict the state or health of high-rate dynamic systems could be invaluable to mitigate intolerable costs of human life or economic loss resulting from unintended failure[1]. If the system is capable of identifying and adapting to the change in a timely manner, control decisions, such as active mitigation strategies, can be undertaken to prevent further damage and complete failure[2].

Advances in estimation and control theory, along with computer sciences, enables the development of observers with rapid convergence for estimation. Such observers have the potential to produce smarter, safer, and more effective systems capable of responding to real-time events. While conventional estimators are not robust to noise and uncertainty, algorithms have been developed to handle such complexities although not without penalties[3]. In the presence of noise, a Kalman Filter (KF)-type observer can be used to obtain accurate estimates, but with added computational costs. Likewise, methods have been developed to overcome heavy computation such as the Uniform Robust Exact Observers (UREO)[4], objective functions formulated from

modal data[5] and self-tuning fusion Kalman filters[6]. Through these efforts, it is undeniable that modern research in state estimation has been geared towards producing faster and more efficient observers for systems with various levels of complexity.

With the growing number of applications needing estimators on high-rate dynamic systems, the research area of state estimation will soon require algorithms that can robustly estimate the states of high-rate dynamic systems. The objective of this paper is to illustrate the importance of addressing the high-rate dynamics-specific challenges, with a particular attention on the importance that the input space of an observer may play in high-rate dynamics state estimation.

Important challenges in high-rate dynamic systems will be introduced. A path to high-rate state estimation is discussed, which leverages adaptive observers (AO) as a promising solution for complex nonstationary systems. The influence of the input space on a high-rate state estimator will be studied, and it will be shown that its proper design can substantially enhance the performance of AO. This investigation will be conducted through simulations of a neuro-observer on high-rate laboratory experimental data.

2 | APPLICATIONS FOR STATE ESTIMATION OF HIGH-RATE DYNAMICS

As scientists and engineers are continually developing faster and more powerful mechanical and civil systems, the concerns for safety is also growing. High-rate systems operate at speeds faster than human reflexes. Thus, in order to operate safely, they require the incorporation of smarter systems capable of making decisions that will protect the lives of the operators and/or surrounding personnel, as well as the financial investments in these high-rate systems. This section discusses engineering systems for which state estimation of high-rate dynamics can be particularly useful. Examples include civil structures exposed to blast, space shuttle debris prone to debris strikes, and aerial vehicle experiencing in-flight changes. They are organized into two categories: 1) impact detection and mitigation; and 2) in-flight monitoring and rapid guidance adaptability.

2.1 | Impact Detection and Mitigation

Designing structures to withstand blast is a growing area of research due to the increased number of terrorist attacks. Military installations are not the only targets as seen in the historical bombings on civilian buildings such as the World Trade Center in 1993 and the Alfred P. Murrah Federal Building in 1995. Sources of blast loads for civil structures are not limited to terrorist attacks, but also include accidental explosions caused by gas leaks, vehicular accidents, and chemicals mishaps. Blast creates a shock wave of energy that often exceeds the yield strength of the structural material, causing damage and jeopardizing structural integrity, and may result in partial or total collapses. Blast mitigation is typically conducted by passive strategies, including friction elements, laminated windows, hardened concrete, and more[7,8,9]. Semi-active and active control methods are also being investigated.

An example of an active blast mitigation method can be found in[10]. The authors proposed a pre-compressed cellular material that deploys before the blast wave arrival. The blast is detected by electromagnetic emission sensors milliseconds before arrival. The compressed material is then deployed by high-speed actuators. The compressibility of the material absorbs the shock waves and the deployment of the material causes momentum cancellation. This active method is preferred over passive methods because it allows blast mitigation using far less materials. While simulations showed promise, it was acknowledged that the release of the cellular material just prior to the arrival of the blast impulse would significantly improve the performance of the proposed procedure. The engineering of such reactive system would require the development of state estimators of high-rate dynamics. Specifically, the arrival time of a blast produced by a 10 kg TNT varies from approximately 0.3 ms at a 1 m range to approximately 100 ms at a 40 m range. It follows that the reactive system would necessitate sensing, estimation, and actuation below this 0.3 - 100 ms range.

Another example of technology for impact detection and mitigation is airbag systems. According to the United States Census Bureau, in 2009 10.8 million motor vehicle accidents occurred of which 30,797 where fatal[11]. Not all accidents lead to serious injuries, but of the ones that do, airbags have played an important role in saving many lives[12]. The airbag control unit uses a combination of sensors such as accelerometers, impact sensors, wheel tachometers, and brake pressure sensors to make a quick decision on whether to deploy the airbags or not. The sensor signals enter an amplifier and are filtered before reaching the airbag control unit. Typical modern systems use threshold levels for each sensor. If the threshold is met for multiple sensors, the airbags trigger. However, at times, airbag systems are known to cause unnecessary or even fatal injuries[13].

Improving the airbag system is ongoing research. For instance, research in[14] on stereovision-based sensing methods uses stereo cameras combined with an intelligent algorithm to determine the occupant classification (small child or unsafe position)

before the deployment of airbags. To accommodate for the large distortions in the data, a thin plate spline algorithm is used to calculate a smooth function and interpolate a surface. The child detection is conducted at the moment the vehicle is started to save on computation time. On the other hand, the unsafe position has to be identified during the impact while determining whether to disable or trigger the airbags in time. This system boasts a processing time of 960 ms. Another area that is being researched is in adaptive airbag deployment. This technology focuses on deployment force, deployment geometry, and stiffness of the airbag using multi stage inflators and venting systems[15]. Fatal accidents occur at a very fast rate, forcing the human body to collide with the interior of the vehicle in a fraction of a second[16]. Like systems which may experience impact conditions could benefit from state estimators capable of estimating high-rate dynamics. In the case of airbag systems, estimation of the high-rate dynamics or impact location of a human-being could result in rapid mitigation decisions to minimize or eliminate damage and losses by appropriate airbag deployment.

2.2 | In-Flight Monitoring and Rapid Guidance Adaptability

Debris strike during a space shuttle launch can be catastrophic. The loss of Columbia in 2003, killing all crew members, arose from the impact of foam insulation to the leading edge of the left wing during the shuttle launch that caused a breach in the thermal protection system. The foam insulation separated 81.7 s into the flight at an altitude of 66,000 ft and traveling at a velocity of 705 m/s[17]. During re-entry, heat pierced the leading-edge insulation which degraded the structure of the left wing. This resulted in a weakening of the structure causing loss of control and eventually destruction of the Orbiter[18]. If the damage had been detected the instant it occurred, the launch could have been aborted, avoiding the catastrophic failure. Since then, NASA has developed and uses a NASA debris radar system to target and track debris during ascent. The NASA debris system automatically detects and characterizes debris. It is capable of assigning a ballistic number to assess the material type, size, release location, and threat associated with the object[19]. While this system is very sophisticated, it uses an offsite ground radar system. Ground intervention is not always possible due to communication delays or visibility issues, and knowledge of failures is required onboard for operational capabilities[20]. Because of the rate at which space shuttles travel during launch and re-entry, even soft materials such as insulating foam behave differently and can pierce through metal panels which may be very difficult to comprehend. Nonetheless, these phenomenons are real and estimators to observe systems under high-rate events are necessary.

More generally, during a flight, aircrafts can experience system failures or damage arising from the failure of components or from an impact with a foreign object such as a bird strike, hail impact, and lightning strike. Such events can cause larger issues if it leads to uncertainty in the navigational decision-making capabilities. In the event of an in-flight failure or damage, rapid estimations using uncertain data are required to regain and maintain control of the aircraft. The faster the estimator, the less the error it needs to compensate for. There has been significant research towards Fault Detection, Isolation and Recovery (FDIR) and prognostics health management sub-systems[21]. The traditional approach to providing fault estimation for aircraft has been to duplicate the hardware such as sensors, actuators, and flight control computers. An alternative to this redundancy is to use a model-based fault detection and diagnosis and generate redundant estimates of measured signals. To achieve robustness in the model-based methods, different techniques have been studied to include optimization methods, unknown input observers, sliding mode observers, and geometric design approaches[22].

Additionally, aerospace technology is moving toward the development of hypersonic passenger and military airframes, which will most likely face similar challenges of foreign object impacts. A typical Boeing passenger aircraft can operate at about 600 mph or equivalently about Mach 0.8. By definition, hypersonic refers to speeds of Mach 5 or greater[23]. High-rate estimators would have the benefit of increasing reaction time to anomalies by allowing faster decisions, decreasing risks associated with system failure. For example, Mach 5 at an altitude 10000 m and -50 °C corresponds to an approximate speed of 1500 m/s. If sampling at 1 Hz, there would be 1500 m travel distance between data points. Alternatively, to obtain a 1 mm resolution while traveling, a sampling rate of 1.5 MHz would be necessary. At such a rate, for each sample an observer requires to converge, the vehicle travels 1 mm. And after the convergence of the observer, there will be time delays for decision making computation and actuator reaction times. Using the input space of a system, we can reduce the number of data points required for convergence and increase the decision speed for monitoring and controlling the high-rate system.

3 | CHALLENGES ASSOCIATED WITH STATE ESTIMATION OF HIGH-RATE DYNAMICS

Estimating the dynamics states of complex structures with high-rate dynamics is a non-trivial task. By definition, high-rate dynamic systems require rapid state estimation to optimize guidance and save lives. Moreover, fast estimators should not be confused with state estimation of "fast" dynamics. For example, state observers for induction motors capable of convergence in the micro-second range have been reported in literature using an adaptive sliding observer and an Extended Kalman Filter (EKF) with computation times of 19 μs and 86 μs, respectively for one update using a 250 MHz processor[24], and using a LO, Sliding Mode Observer (SMO), and EKF with computation times of μs, 5 μs, and 100 μs, respectively for one update using a 150 MHz processor[25]. While this demonstrates that microsecond state estimation is possible and currently exists for some applications, the induction motor itself is not a high-rate dynamic system but instead a "fast" dynamic system. There are three key factors that differentiate high-rate dynamic systems from fast dynamic systems. High-rate dynamic systems may have:

- Large uncertainties on the external loads. High-rate events will occur at an undetermined time with an uncertain amplitude. For example, a man-made blast cannot be predicted in time and its amplitude largely depends on the explosive used and the detonation distance.
- High levels of nonstationarity and heavy disturbance. A high-rate load may provoke large changes in the system's states, and could also significantly alter the system's dynamic parameters. For example, an unmanned aerial vehicle could lose a wing following a debris strike.
- Generation of unmodeled dynamics (noise) from change in mechanical configuration. The exposure to highly dynamic environments can cause significant changes which can appear as noise in measurements. For example, noise may arise from cable movement, flexing of the electronics, and threaded interfaces which may rattle from loss of torque under high amplitude dynamics.

These factors seen in the form of system complexities (e.g., uncertain systems, noisy systems, etc.), have been considered in many research, and solutions to specific complexities have been proposed[5,6,26,27,28,29,30]. Nevertheless, research is yet to address situations when all of these factors are combined, also known as the high-rate dynamics problem.

3.1 | A Path to State Estimation of High-Rate Dynamics

Further developments and extensions of state-of-the-art fixed and adaptive observers need to be conducted in order to broaden the applicability of observers to the problem of state estimation of high-rate dynamic systems. While many paths could be undertaken to achieve that goal, the authors are noting the particular promise of adaptive data-based observers. AOs have been proposed to estimate the unmeasurable states for different classes of nonlinear systems[31]. They are typically characterized by asymptotic stability[32], but are known to have slower convergence rates. In related studies, reference[32] attributed this problem to the utilization of single observation errors, while reference[31] explained this slow convergence by the complexity of the adaptive law. AOs can be used to estimate states and parameters using input-output measurements, ideal for handling uncertainty in state estimation[33]. Methods include fuzzy logic[34] and neural network (NN) estimators[35]. The performance of data-based method is linked to the quality of data mining and interpretation algorithms, and an additional limitation can be found in the computational time required to achieve an appropriate estimate[36].

The adaptable characteristics of a state estimator is deemed critical for high-rate dynamic systems given the high levels of uncertainties, nonstationarity, disturbance, and noise that they can undergo. Data-based solutions can also be particularly helpful at providing important flexibility by enabling state estimation without the reliance on a model, in particular for highly uncertain and nonstationary systems. For dynamic parameters undergoing large variations, a hybrid form between data- and model-based solutions could be used to accelerate convergence. For instance, a data-based technique would be used as a system identifier fed into a model-based technique. It follows that, while the authors selected an adaptive data-based approach as a possible path to the high-rate state estimation challenge, other viable techniques exist. Examples include dual methods of system identification and state estimation using KFs for time varying systems[37], modal-based methods including numerical algorithms for subspace state space system identification[38] and eigensystem realization algorithm[39], and statistical methods including particle filters[40] and unscented Kalman filters[41].

The data-based adaptive state estimators are in essence black-box models that could be pre-trained or adapted sequentially. In the high-rate dynamics problem, pre-training could be difficult for a certain set of systems given the uncertainty on external

loads. Sequential adaptation is also challenging, because the system is required to learn and perform on-the-spot. Algorithms capable of sequential adaptation and immediate performance have been studied in the field of structural control for mitigation of unknown excitations in uncertain systems [42,43]. However, sequential adaptation will typically yield larger initial errors and a slower convergence rate, and it follows that such observer needs to be designed appropriately.

The sequential adaptive learning problem can be simplified as the construction of a function characterizing an input-output system. This problem has been researched and addressed in many fields through various machine learning methods. When looking at high-rate dynamic systems as input-output systems, a key feature that distinguishes them is the vast quantity of input data. Even in the case of a single sensor, the very large sampling rate will result in the accumulation of a vast time series vector. It results that one needs to decide which part of this time series would be fed as input, or how many delayed observations will constitute the inputs such as:

$$\begin{aligned}\hat{y}_k &= f(y_i(t), y_i(t-\tau), y_i(t-2\tau), \cdots, y_i(t-(d-1)\tau)) \\ &= f(\nu(\tau, d))\end{aligned} \tag{1}$$

where $\hat{y}_k$ is the estimated state, y_i is an observation i, τ is a time delay, and d is the dimension of the input space ν, with ν termed the delay vector [44]. These parameters must be selected carefully in order to guarantee a certain level of performance. The procedure to select an input space in data-based techniques is often overlooked. The selection of input may influence computation time, adaptation speed, effects of the curse of dimensionality, understanding of the representation, and model complexity [45,46,47,48]. Available selection techniques include the filter methods, where the input selection is independent of the black-box model [49], the wrapper methods, where the results from the black-box model are used to rank and select the inputs [50], and the embedding methods, where selected inputs are used for adapting the representation [51]. Automatic input selection methods have been discussed [52,53,48,54,55], but they are traditionally applied offline and necessitates pre-training. In the case of high-rate dynamic systems, as it will be demonstrated in the next section, the selection of the input space is critical to the observer's performance, and the optimal input space varies as a function of events.

4 | STUDY OF SYSTEM INPUT SPACE

We demonstrate the importance of the input space selection for high-rate dynamic systems by designing a neuro-observer and evaluating its performance as a function of different inputs. The design of the neuro-observer is presented in detail below. The subsequent subsection presents and discuses results from the simulation of the state estimation of a system experiencing high-rate dynamics. Note that the design of the neuro-observer was kept simple in order to focus the discussion on the importance of the input space selection. One could certainly design an adaptive observer that would provide, overall, better performance.

4.1 | Neuro-observer Architecture

The neuro-observer is a single-layer wavelet neural network written

$$\hat{y}_k = \sum_{j=1}^{h} \gamma_j \phi_j(\boldsymbol{\nu}) \tag{2}$$

where h represents the number of nodes, γ the nodal weights of node j, and ϕ is the activation function taken as a Mexican hat wavelet

$$\phi(\boldsymbol{\nu}) = \left(1 - \frac{\|\boldsymbol{\nu} - \boldsymbol{\mu}\|_2}{\boldsymbol{\sigma}^2}\right) e^{-\frac{\|\nu-\mu\|_2}{\sigma^2}} \tag{3}$$

where $\boldsymbol{\mu}$ and $\boldsymbol{\sigma}$ are the wavelet centers and bandwidths, respectively, and $\|\cdot\|_2$ is the 2-norm. The neuro-observer is designed to be capable of sequential adaptive learning, whereas no prior training is necessary. To do so, a self-organizing mapping architecture is adopted to minimize the network size [56]. This self-organization is conducted by adding a node if a new observation falls outside an Euclidean distance threshold D to the closest node. When a new node j is added, it is given a weight γ_j initially equal to zero, a center $\boldsymbol{\mu}_j$ at the location of the new observation, and bandwidth $\boldsymbol{\sigma}_j$ of the newly added wavelet initially set at 10000.

The network is then put in an adaptation mode, where weights and bandwidths are adapted following a back-propagation rule. With the back-propagation rule, an adaptive parameter ζ is varied using

$$\dot{\zeta} = \Gamma_{\zeta} \frac{\partial(\boldsymbol{\gamma}^T \boldsymbol{\phi})}{\partial \zeta} \tilde{y} \tag{4}$$

where $\tilde{y}$ is the observation error between the estimated and the measured state and Γ_{ζ} is the learning rate associated with the adaptive parameter ζ. The stability of the adaptation rule has been derived in [43]. In a discrete notation, Eq. (4) can be specialized for $\boldsymbol{\mu}_j$ and $\boldsymbol{\sigma}_j$ at node j:

$$\begin{aligned} \gamma_j(k+1) &= \gamma_j(k) - \Gamma_{\gamma_j} \phi_j(\boldsymbol{v}) \tilde{y} \\ \sigma_j(k+1) &= \sigma_j(k) - \Gamma_{\sigma_j} \gamma_j \left(\frac{1}{\sigma_j^5} \mathrm{e}^{\frac{-\|\boldsymbol{v}-\mu_j\|^2}{\sigma_j^2}} (4\sigma_j^2 \|\boldsymbol{v}-\mu_j\|^2 - 2\|\boldsymbol{v}-\mu_j\|^4) \right) \tilde{y} \end{aligned} \tag{5}$$

where k is a discrete time step.

4.2 | Simulations

Simulations of the estimation using the neuro-observer were conducted on experimental data collected from an impact test series conducted on an electronic components package to demonstrate the importance of proper input space selection. The experimental setup is illustrated in Fig. 1 . On the right is the electronics system of interest. The systems contains four circuit boards, each of the four boards have a surface mounted high-g shock accelerometer (Meggitt 72). These accelerometers are capable of accurately measuring acceleration upwards of 120,000 g_n or 120 kg_n [57]. The circuit boards are housed in a metal canister and filled with an electronics potting material. The system is secured in a metal fixture, shown in the middle of the figure, using a lock ring. On the left is the MTS-66 drop tower designed to generate a prescribed impact condition. Bungee cords are used to accelerate the table of the drop tower. The fixture housing the system is mounted on the drop tower table using bolts. The picture shows the table in the raised state. When the table brakes are released, the table along with the system accelerates downward and impacts the black mass at the bottom of the drop tower creating a mechanical shock. In this section, the acceleration data is presented in terms of g_n (1 $g_n = 9.81$ m/s$^2 = 32.2$ ft/s^2).

This problem contains many complexities making model-based techniques difficult to apply. The accelerometers are hard-wired to the data acquisition system. When the table accelerates, so does the sensor cables, creating a violent whipping motion.

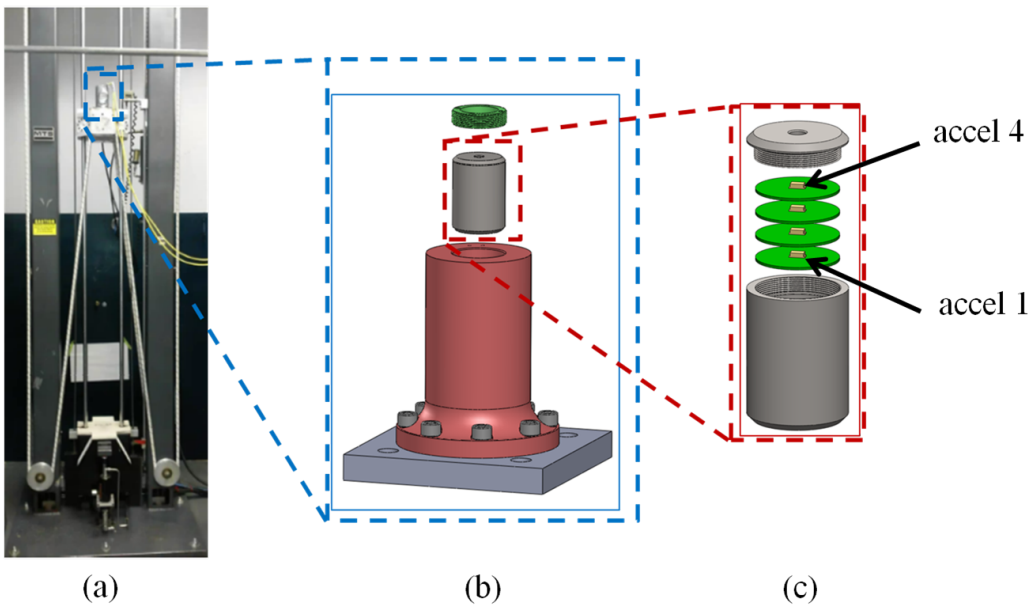

FIGURE 1 Experimental setup: (a) MTS-66 drop tower, (b) unit fixture, (c) electronics unit.

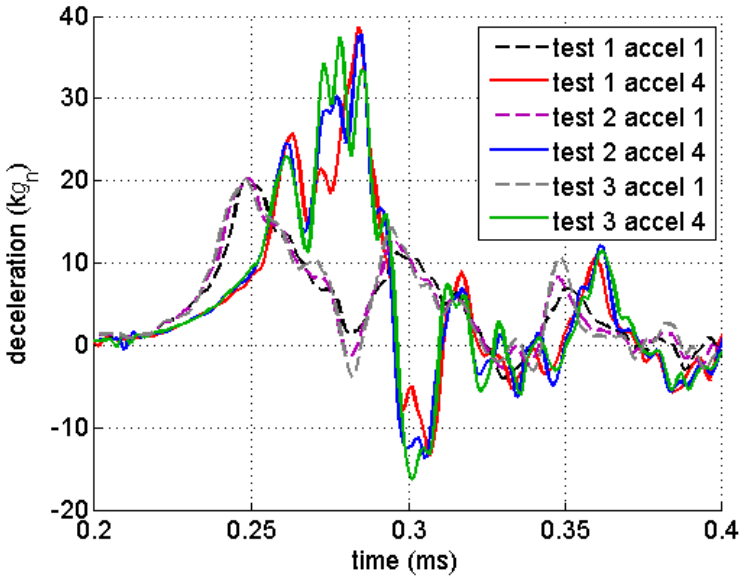

FIGURE 2 Response of three subsequent tests.

Even though careful selection of cables was made, some noise is added from whipping of the cables. Additionally, whenever metal parts are coupled together in impact scenarios, such as in this case, noise is produced from the chattering of the parts. Uncertainties associated with this problem include unknown material high-rate response of the circuit boards and potting material, uncertainties in the exact placement of the accelerometers and circuit board spacing, and boundary conditions such as whether or not the potting material moves in relation to the housing. The exact input to the system resulting from the table impact is unknown. Only the measurement from the response of the accelerometers can be taken as certain. Note that such tests are considered as small impact tests within the shock dynamics community, and not enough energy was present to excite the sensor resonance. However, it is not uncommon in larger impact tests to notice disturbances created from sensor and/or system resonance.

The studied system bears many characteristics of a high-rate system. The way data is used in the simulation greatly simplifies the problem significantly by attempting to identify a representation estimating accel 4 using accel 1, where the inputs and outputs are the systems are known. Typical field applications would either have the outputs be unknown, for instance the estimation of velocity for acceleration data, or use the inputs to conduct system identification, for instance the identification of a stiffness value. Such realistic applications require the integration of additional steps and mathematics in the algorithm, which would drive the attention away from our discussion on the opportunities and limitations in the input space.

The impact is controlled by specifying a drop height and mitigating material. Event 1 is created with a drop height of 20 in and 1/16 in thickness felt. The raw data was collected using a National Instruments PXI-6133 High-Speed cards with a sampling rate of 1 MHz coupled with a Precision Filters signal conditioning system 28144A quad-channel wideband transducer conditioner with an anti-aliasing filter of 204.6 kHz. Figure 2 shows three back-to-back tests of event 1 that exhibit gradual increases in the response pointing to time varying parameters possibly from the weakening of the glue that holds the accelerometers on to the circuit boards and/or from the electronics potting material de-bonding from the internal walls of the unit's metal canister. This confirms the high-rate dynamic nature of our system.

Figure 3 shows the experimental data from accelerometers 1 (accel 1) and 4 (accel 4) of test 2, which the simulations of the estimation using the neuro-observer are conducted on. These accelerometers are selected because of the notable difference between the two responses. The impact occurs over 0.1 ms starting at about 0.2 ms, which in turn excites the system that responds over the next 0.6 ms. In the course of the dynamic event, an acceleration level greater than 60 kg_n is observed.

In the simulations, accel 1 was used as the input and accel 4 was used as the output. The input was used to estimate the output using the neuro-observer. For the investigation, a lower rate event was synthetically created by filtering the experiment data at 5 kHz using a 4-pole Butterworth low pass filter, with the purpose to demonstrate the added importance of the input space for high-rate systems. From here on, high-rate data will refer to the raw data and low-rate data will refer to the filtered data. Both time series are plotted in Fig. 4 .

Two different metrics were used to quantify the performance of the input space. The first performance metric J_1 of the estimator is taken as

$$J_1 = \frac{\|(\hat{\mathbf{y}} - \ddot{\mathbf{x}}_4)\|_2}{\|\ddot{\mathbf{x}}_4\|_2} \tag{6}$$

with $\hat{\mathbf{y}} = \hat{\ddot{\mathbf{x}}}_4$ being the estimation of the measurement of accel 4, $\ddot{\mathbf{x}}_4$. The $\|\cdot\|_2$ represents the 2-norm. By representing the error of the estimate as described in equation 6, the error is normalized to fall within the values of [0,1]. Additionally, normalizing the error helps to compare the errors between various simulations.

The second performance metric J_2 of the estimator is in terms of the convergence rate. The convergence rate is defined as the time it takes from the start of the impact (>100 g_n) to when the estimation error falls and remains within an error threshold. The error threshold was determined to be 5% and is governed by the variations in the data created by the experimental setup. Because the objective of the paper is to demonstrate the importance of the input space and not the optimality of the observer solution, the computational time is used as a performance metric. For the same reason, a study on the influence of internal parameter tuning is not conducted. Here, the internal parameters Γ_σ, Γ_γ, and the initial γ and σ were tuned based on a prior study from the authors presented in [58].

A parametric study of the input space in terms of the embedding dimension and time delay was conducted on both the high- and low-rate data. The parametric study was conducted by running the estimator over a grid of possible input space $d = [2{:}1{:}10]$ and $\tau = [1{:}1{:}400]$ to find the optimal values for d and τ (Eq. (1) that minimized J_1). We find $d = 3$ and $\tau = 46$ for the high-rate data, and $d = 2$ and $\tau = 150$ for the low-rate data. The fitting errors using these values are plotted in Fig. 5 . It can be noted that the optimal dimension d decreases with a smoother function (e.g., low-rate data), and that the smoother function leads to a significantly lower estimation error, yielding $J_1 = 0.238$ for the high-rate data, and $J_1 = 0.106$ for the low-rate data. Also, the estimator for the filtered data converges 0.105 ms faster. The lower performance of the estimator on the raw data is explained by the larger and higher nonlinearities in the estimated dynamics.

The influence of the input space on the performance of the estimator is further studied by investigating different combinations of d and τ. The combinations and associated performance J_1 and J_2 are listed in Table 1 , in which the change in performance, or percent difference in J_1 and J_2 relative to the optimal performance is indicated in columns 6 and 8 respectively. Note that a dimension $d = 2$ is considered as the lowest possible dimension, and therefore the under embedding is not shown for the low-rate data.

Results from Table 1 shows that utilizing the wrong input space for the high-rate dynamics results in larger decreases in performance J_1 when compared to the utilization of the wrong input space for the low-rate dynamics. This is similar for the J_2 performance metric, except for the effect of over embedding which is important for both the high- and low-rate systems, yet

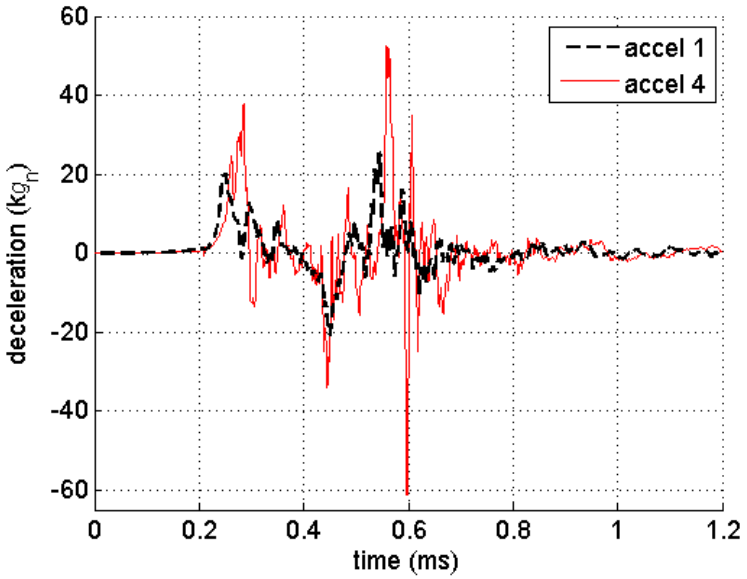

FIGURE 3 Experimental data from the accelerometer measurements.

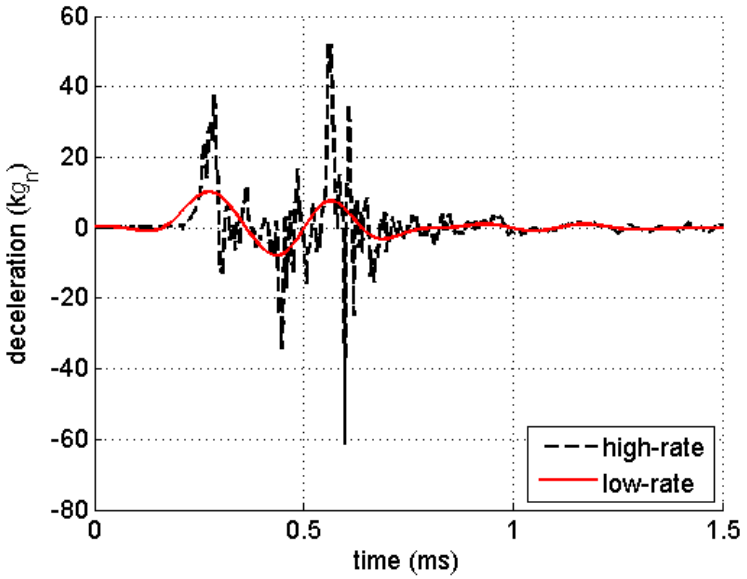

FIGURE 4 High and low rate data the simulations were conducted on.

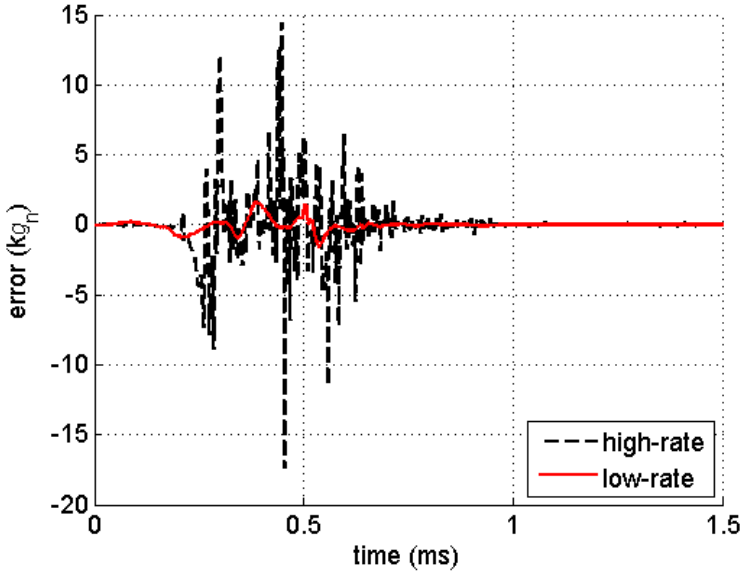

FIGURE 5 Comparison between estimation errors of high- and low-rate data.

larger for the low-rate system. For the high-rate dynamics, under embedding yields to a better performance when compared to over embedding. This can be explained by a faster convergence provided by a lower input space dimension, because a function of lower dimension can be populated faster with sequential training examples. Using the wrong τ has dramatic effects on the performance of the high-rate estimator. Fig. 6 is a plot of the absolute estimation errors of the high-rate dynamics under different input spaces. The absolute estimation error is used to portray the errors associated with incorrect input spaces to make the plots more readable. An input space of incorrect time delay ($d = 3$, $\tau = 150$) yields a significantly higher error peaks compared to other strategies. Under embedding ($d = 2$, $\tau = 46$) produces a large error peak at about 0.6 ms, same as for the incorrect time delay but around 50% lower in magnitude. Over embedding ($d = 4$, $\tau = 46$) also results in high peaks, yet of relatively smaller magnitude. The error peak at 0.6 ms is about equal to the under embedding error and the other peak occurs after the convergence

TABLE 1 Estimator performance associated with different input spaces.

data	combination	d	τ	J_1	% diff J_1	J_2 (ms)	% diff J_2
high-rate	optimal	3	46	0.238	–	0.484	–
high-rate	under embedding	2	46	0.310	30.3	0.542	12.0
high-rate	over embedding	4	46	0.454	90.8	0.876	81.0
high-rate	incorrect information	3	150	0.441	85.3	0.681	40.7
low-rate	optimal	2	150	0.106	–	0.379	–
low-rate	over embedding	3	150	0.143	34.9	0.748	97.4
low-rate	incorrect information	2	46	0.141	33.0	0.446	17.7

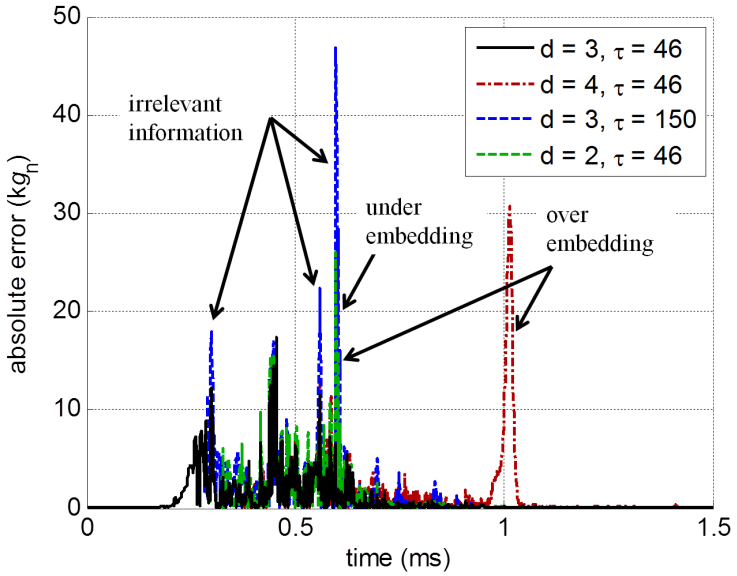

FIGURE 6 Absolute estimation errors for different input strategies for high-rate dynamics.

with the other strategies. The presence of these abnormal high error peaks can lead to false alarms and incorrect decisions in the closed-loop process.

Figure 7 shows how the convergence rate is affected by the choice of different d and τ. The results show that different input spaces within the provided range can yield a difference in convergence rate over 1 ms, which is very large for high-rate dynamics. Note that a convergence rate beyond 1.5 ms means that the estimator never converged and the simulation was stopped, because the high amplitude dynamic response is approximately 1 ms. The optimal convergence rate is given by the choice $d = 3$ and $\tau = 27$ yielding a convergence rate of 0.467 ms (a 3.5% increase in performance), which differs from the input space providing the best 2-norm error (J_1) and yields $J_1 = 0.316$ (a 32.8% decrease in performance). The choice of lower dimensions d generally yield a more constant convergence rate for varying τ.

TABLE 2 Optimal d and τ for events 1 and 2.

dynamic event	combination	d	τ	J_1	% diff J_1	J_2 (ms)	% diff J_2
event 1	optimal	3	46	0.238	–	0.484	–
event 1	incorrect	4	54	0.435	82.8	1.027	112.2
event 2	optimal	4	54	0.196	–	0.490	–
event 2	incorrect	3	46	0.256	30.6	0.637	30.0

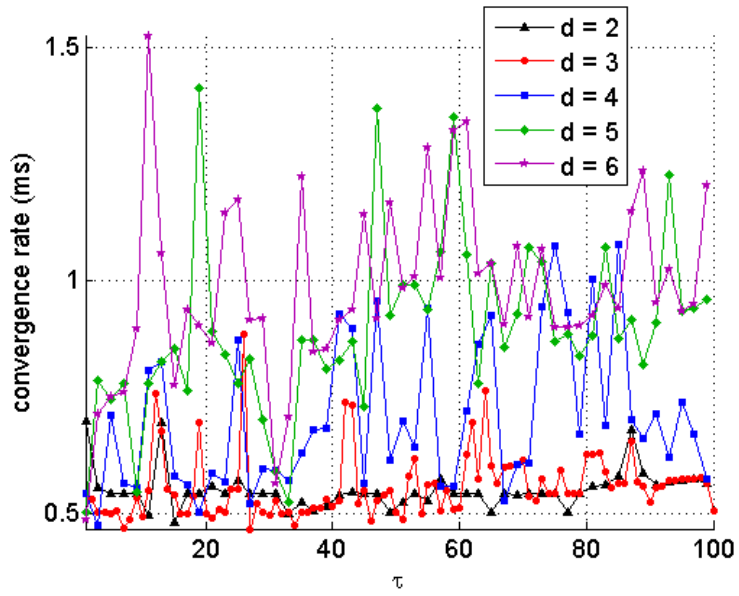

FIGURE 7 Convergence rates as a function of embedding dimensions and time delays for high-rate dynamics.

Simulations of the estimation using the neuro-observer were also conducted on experimental data from a second impact event. The second impact event was created with a drop height of 72 in and 1/2 in thickness felt, instead of a drop height of 20 in and 1/16 in thickness felt for the first impact. In reality, different environmental conditions could occur even from a slight change in impact location or angle, for example, that can produce very different results by exciting different modes with different phases. The optimal input space was determine for both events, independently. Figure 8 shows the different dynamic events.

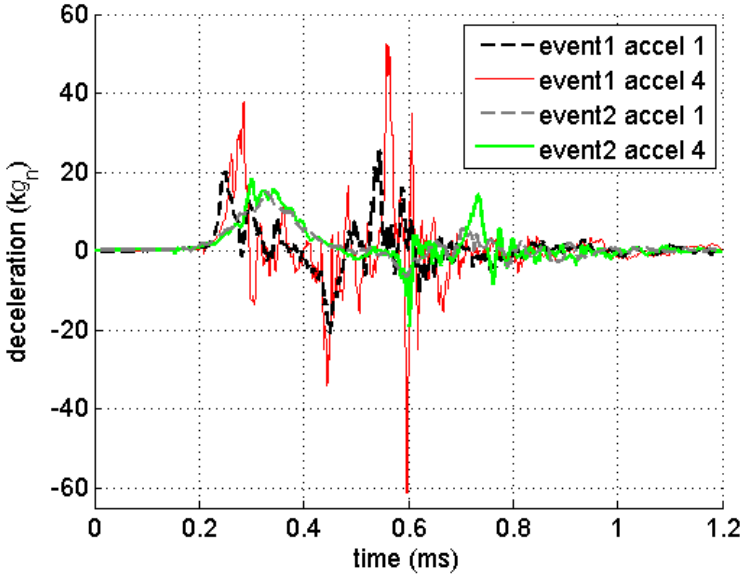

FIGURE 8 Dynamic event 1 and 2.

The optimal d and τ for event 1 and 2 are listed in table 2 .

The performance attained using optimal input space, optimized for the J_1 metric, for events 1 and 2 were compared. Results are listed in Table 2 . Using the optimal input space of event 1 for event 2, there is a 30% decrease in performance for both J_1 and J_2. A significantly worst result is observed seen when using the optimal input for event 2 for event 1. These results show

that while an static input space could be designed based on an event, it might be very ineffective when used for state estimation of the same system subjected to a different event.

5 | CONCLUSION

State estimation of high-rate dynamics is a challenging task, in particular for complex engineering systems experiencing highly dynamic events and requiring real-time observability to ensure adequate performance. Application of the estimators on the high-rate systems include hypersonic vehicles and impact protection systems. High-rate system state estimation-specific challenges were listed, and the applicability of typical observers at achieving that specialized task discussed. A path to state estimation of high-rate dynamics was presented. It was argued that data-based adaptive observers (AOs) could be particularly promising, because of their ability to process information without knowledge of system dynamics or the high-rate event, and their high adaptability to complex dynamics. However, the utilization of AOs comes with the cost of slower convergence rates, a critical obstacle to the state estimation of high-rate dynamics problem.

A potential solution to improving the convergence rate of AOs is through the careful design of the input space of the estimator. The influence of the input space on a high-rate state estimator was investigated. An adaptive neuro-observer was constructed and simulations were performed on high-rate laboratory experimental data. The estimator's performance was based on the normalized 2-norm errors and convergence rates. Simulation results highlighted a few key observations:

- The use of a proper input space is critical to enhancing the performance of high-rate dynamics state estimators. The use of incorrect input space for estimation has significant negative impacts, which are much larger for high-rate data than low-rate data.
- The misrepresentation of the system dynamics through wrong input spaces produces abnormally large error peaks, which can lead to poor decisions in the closed-loop process.
- The input space is not unique to a system, but rather to a dynamic environment. Different input spaces are required for different events for optimal estimator performance.

From the simulation results, the importance of input space in evident in making the most accurate and fast estimations. The challenge is choosing the right input space for the right situation. Often, the type of high-rate dynamic event a system will experience before the event occurs is unknown, and pre-selecting the input space is a very challenging task. A solution, part of future work, is to develop algorithms automating the input space selection process as a function of different events, yielding adaptive input spaces.

5.1 | Acknowledgements

The authors would like acknowledge the financial support from the Air Force Research Laboratory (AFRL) RW Chief Scientist office under the guidance of Dr. Jason Foley, from the Air Force Office of Scientific Research (AFOSR) award number FA9550-17-1-0131, and AFRL/RWK contract number FA8651-17-D-0002. Additionally the authors would like to acknowledge Dr. Janet Wolfson for providing the experimental data. Opinions, interpretations, conclusions and recommendations are those of the authors and are not necessarily endorsed by the United States Air Force.

References

[1] R. Lowe, J. Dodson, and J. Foley, "Microsecond prognostics and health management", IEEE Reliability Society Newsletter **60**.

[2] Jerome Connor and Simon Laflamme, Structural Motion Engineering, Springer International.

[3] S Mondal, G Chakraborty, and K Bhattacharyya, "Robust unknown input observer for nonlinear systems and its application to fault detection and isolation", Journal of Dynamic Systems, Measurement, and Control **130**(4), pp. 1–5 (2008).

[4] Liset Fraguela, Marco Tulio Angulo, Jaime Moreno, and Leonid Fridman, "Design of a prescribed convergence time uniform robust exact observer in the presence of measurement noise", In IEEE 51st Annual Conference on Decision and Control , pp. 6615–6620. IEEE (2012).

[5] Seyed Sina Kourehli, Abdollah Bagheri, Gholamreza Ghodrati Amiri, and Mohsen Ghafory-Ashtiany, "Structural damage detection using incomplete modal data and incomplete static response", KSCE Journal of Civil Engineering **17**(1), pp. 216–223 (2013).

[6] Gui-Li Tao and Zi-li Deng, "Convergence of self-tuning riccati equation for systems with unknown parameters and noise variances", In 8th World Congress on Intelligent Control and Automation (WCICA) , pp. 5732–5736. IEEE (2010).

[7] Lorraine H Lin, Eve Hinman, Hollice F Stone, and Allison M Roberts, "Survey of window retrofit solutions for blast mitigation", Journal of Performance of Constructed Facilities **18**(2), pp. 86–94 (2004).

[8] Ye Zhengqiang, Li Aiqun, and Xu Youlin, "Fluid viscous damper technology and its engineering application for structural vibration energy dissipation", Journal of Southeast University (Natural Science Edition) **32**(3), pp. 466–473 (2002).

[9] Eve Hinman, "Blast safety of the building envelope", Whole Building Design Guide, National Institute of Building Sciences (2005).

[10] Haydn NG Wadley, Kumar P Dharmasena, MingYuan He, Robert M McMeeking, Anthony G Evans, Tan Bui-Thanh, and R Radovitzky, "An active concept for limiting injuries caused by air blasts", International Journal of Impact Engineering **37**(3), pp. 317–323 (2010).

[11] "Transportation", https://www.census.gov/library/publications/2011/compendia/statab/131ed/transportation.html (2012).

[12] B. Meier, "Study shows air bags save lives, but says seat belts are needed, too".

[13] K Cunningham, TD Brown, E Gradwell, and PA Nee, "Airbag associated fatal head injury: Case report and review of the literature on airbag injuries", Journal of Accident & Emergency Medicine **17**(2), pp. 139–142 (2000).

[14] S-J Lee, M-S Jang, Y-G Kim, and G-T Park, "Stereovision-based real-time occupant classification system for advanced airbag systems", International Journal of Automotive Technology **12**(3), pp. 425–432 (2011).

[15] "Trw introduces adaptive airbags".

[16] Romania Din, "Injuries of the foot and ankle joint and their mechanisms", Societatea Inginerilor de Automobile (2004).

[17] James D Walker, "From columbia to discovery: Understanding the impact threat to the space shuttle", International Journal of Impact Engineering **36**(2), pp. 303–317 (2009).

[18] D. Smith, "Megalightning and the demise of sts-107 space shuttle columbia: A fresh look at the available evidence".

[19] Brian M Kent, "Return-to-flight electromagnetic measurementsâĂŤthe nasa shuttle ascent debris radar system", In 8th European Conference on Antennas and Propagation , pp. 1–3. IEEE (2014).

[20] Robert Fonod, Catherine Charbonnel, and Eric Bomschlegl, "A class of nonlinear unknown input observer for fault diagnosis: Application to fault tolerant control of an autonomous spacecraft", In UKACC International Conference on Control , pp. 13–18. IEEE (2014).

[21] Youmin Zhang and Jin Jiang, "Bibliographical review on reconfigurable fault-tolerant control systems", Annual Reviews in Control **32**(2), pp. 229–252 (2008).

[22] Xiaoyu Sun, Ron J Patton, and Philippe Goupil, "Robust adaptive fault estimation for a commercial aircraft oscillatory fault scenario", In International Conference on Control , pp. 595–600. IEEE (2012).

[23] "Hyersonic".

[24] Z Xu, F Rahman, and Dianguo Xu, "Comparative study of an adaptive sliding observer and an ekf for speed sensor-less dtc ipm synchronous motor drives", In Power Electronics Specialists Conference , pp. 2586–2592. IEEE (2007).

[25] Yongchang Zhang, Zhengming Zhao, Ting Lu, Liqiang Yuan, Wei Xu, and Jianguo Zhu, "A comparative study of luenberger observer, sliding mode observer and extended kalman filter for sensorless vector control of induction motor drives", In Energy Conversion Congress and Exposition , pp. 2466–2473. IEEE (2009).

[26] Rui Manuel Freitas Oliveira, EC Ferreira, Filomena Oliveira, and S Azevedo, "A study on the convergence of observer-based kinetics estimators in stirred tank bioreactors", Korean Institute of Chemical Engineers **6**(6), pp. 367–371 (1994).

[27] Karla Stricker, Lyle Kocher, Dan Van Alstine, and Gregory M Shaver, "Input observer convergence and robustness: Application to compression ratio estimation", Control Engineering Practice **21**(4), pp. 565–582 (2013).

[28] Kou Yamada and Masahiko Kobayashi, "A design method for unknown input observer for non-minimum phase systems", In International Workshop and Conference on Photonics and Nanotechnology , pp. 1–6. International Society for Optics and Photonics (2007).

[29] Yan Wang, Rajesh Rajamani, and David M Bevly, "Observer design for differentiable lipschitz nonlinear systems with time-varying parameters", In 53rd Annual Conference on Decision and Control (CDC) , pp. 145–152. IEEE (2014).

[30] Bong Keun Kim, Wan Kyun Chung, and Kohtaro Ohba, "Design and performance tuning of sliding-mode controller for high-speed and high-accuracy positioning systems in disturbance observer framework", IEEE Transactions on Industrial Electronics **56**(10), pp. 3798–3809 (2009).

[31] Karim Khayati and Jiang Zhu, "Adaptive observer for a large class of nonlinear systems with exponential convergence of parameter estimation", In International Conference on Control, Decision and Information Technologies (CoDIT) , pp. 100–105. IEEE (2013).

[32] Mohammad Shahrokhi and Manfred Morari, "A discrete adaptive observer and identifier with arbitrarily fast rate of convergence", IEEE Transactions on Automatic Control **27**(2), pp. 506–509 (1982).

[33] Yang Yingjuan and Xuan Pengzhang, "Design of a nonlinear adaptive observer for a class of lipschitz systems", In 33rd Chinese Control Conference (CCC) , pp. 2240–2243. IEEE (2014).

[34] Lotfi A Zadeh, "A summary and update of âĂIJfuzzy logicâĂİ", In International Conference on Granular Computing (GrC) , pp. 42–44. IEEE (2010).

[35] B. Derrida, "Introduction to neural network models", Nuclear Physics B **4**, pp. 673–677 (1988).

[36] I Guyon, "Neural networks and applications tutorial", Physics Reports **207**(3), pp. 215–259 (1991).

[37] C. Hu, B. Youn, and J. Chung, "A multiscale framework with extended kalman filter for lithium-ion bettery soc and capacity estimation", Applied Energy **92**, pp. 694–704 (2012).

[38] P. Van Overschee and M. Bart De, "N4sid: Subspace algorithms for the identification of combined deterministic-stochastic systems", Automatica **30**(1), pp. 75–93 (1994).

[39] J. Juang and R. Pappa, "An eigensystem realization algorithm for modal parameter identification and model reduction", Journal of Guidance, Control, and Dynamics **8**(5), pp. 620–627 (1985).

[40] S. Arulampalam, S. Maskell, N. Gordon, and T. Clapp, "A tutorial on particle filters for on-line non-linear/non-gaussian bayesian tracking", IEEE Transactions on Signal Processing **50**(2), pp. 174–188 (2002).

[41] E. Chatzi and A. Smyth, "The unscented kalman filter and particle filter methods for nonlinear structural system identification with non-collocated heterogeneous sensing", Structural Control and Health Monitoring **16**, pp. 99–123 (2009).

[42] Simon Laflamme, Jean-Jacques E Slotine, and Jerome J Connor, "Wavelet network for semi-active control", Journal of Engineering Mechanics **137**(7), pp. 462–474 (2011).

[43] Simon Laflamme, JJ E Slotine, and JJ Connor, "Self-organizing input space for control of structures", Smart Materials and Structures **21**(11), pp. 115015 (2012).

[44] Jonathan Hong, Simon Laflamme, and Jacob Dodson, "Variable input observer for structural health monitoring of high-rate systems", Quantitative Nondestructive Evaluation **43** (2016).

[45] R. Sindelar and R. Babuska, "Input selection for nonlinear regression models", Fuzzy Systems, IEEE Transactions on **12**(5), pp. 688–696 (2004).

[46] G.J. Bowden, G.C. Dandy, and H.R. Maier, "Input determination for neural network models in water resources applications. Part 1–background and methodology", Journal of Hydrology **301**(1-4), pp. 75–92 (2005).

[47] X. Hong, RJ Mitchell, S. Chen, C.J. Harris, K. Li, and GW Irwin, "Model selection approaches for non-linear system identification: a review", International journal of systems science **39**(10), pp. 925–946 (2008).

[48] A. da Silva, P. Alexandre, V.H. Ferreira, and R.M.G. Velasquez, "Input space to neural network based load forecasters", International Journal of Forecasting **24**(4), pp. 616–629 (2008).

[49] A.L. Blum and P. Langley, "Selection of relevant features and examples in machine learning", Artificial intelligence **97**(1-2), pp. 245–271 (1997).

[50] R. Kohavi and G.H. John, "Wrappers for feature subset selection", Artificial intelligence **97**(1-2), pp. 273–324 (1997).

[51] I. Guyon and A. Elisseeff, "An introduction to variable and feature selection", The Journal of Machine Learning Research **3**, pp. 1157–1182 (2003).

[52] DL Yu, JB Gomm, and D. Williams, "Neural model input selection for a MIMO chemical process", Engineering Applications of Artificial Intelligence **13**(1), pp. 15–23 (2000).

[53] K. Li and J.X. Peng, "Neural input selection–A fast model-based approach", Neurocomputing **70**(4-6), pp. 762–769 (2007).

[54] J. Tikka, "Simultaneous input variable and basis function selection for RBF networks", Neurocomputing **72**(10-12), pp. 2649–2658 (2009).

[55] N. Kourentzes and S.F. Crone, "Frequency independent automatic input variable selection for neural networks for forecasting", The 2010 International Joint Conference on Neural Networks (IJCNN) , pp. 1–8 (2010).

[56] Teuvo Kohonen, "The self-organizing map", Neurocomputing **21**(1–3), pp. 1–6 (1998).

[57] A. Beliveau, J. Hong, J. Coker, and N. Glikin, "Cots piezoresistive shock accelerometers performance evaluation", Shock and Vibration Exchange **83** (2012).

[58] J. Hong, L. Cao, S. Laflamme, and J. Dodson, "Robust variable input observer for structural health monitoring of systems experiencing harsh extreme environments", 11th International Workshop on Structural Health Monitoring **11** (2017).

How cite this article: Hong J., L. Cao, S. Laflamme, and J. Dodson (2017), Study of Input Space for State Estimation of High-Rate Dynamics, *Structural Control and Health Monitoring*, *2017;00:1–6*.